PHOTONIC SENSORS / Vol. 10, No. 2, 2020: 113–122

Analysis of Coupled Surface Plasmon in LHM Mediated Dielectric Gap Multilayer Structure

Mohammed BENDJEBBOUR, Abdellatif CHERIFI, and Benamar BOUHAFS*

University of Tlemcen, Faculty of Sciences, Theoretical Physics Laboratory, Tlemcen 13000, Algeria

*Corresponding author: Benamar BOUHAFS E-mail: bouhafs_ben@yahoo.fr

Abstract: The purpose of this work is to investigate theoretically the characteristics of confined electromagnetic modes propagating along the interfaces of a multilayer device. This one dimensional (1D) sensor is formed by stacking a left-handed material (LHM) layer between a SiO_2-glass prism and a dielectric gap layer in contact with gold (Au). The results indicate that the total thickness of the LHM layer and dielectric gap, in optimum conditions, give the ability of tuning significantly the characteristics of the resonant modes correlated to surface plasmons (SPs) propagation along the interfaces of the designed device. By considering two arrangements between LHM and Au, two opposite resonant behaviors observed in p-reflectance spectra are analyzed in the angular interrogation mode and discussed thoroughly.

Keywords: Confined electromagnetic modes; surface plasmon resonance sensor; left-handed material

Citation: Mohammed BENDJEBBOUR, Abdellatif CHERIFI, and Benamar BOUHAFS, "Analysis of Coupled Surface Plasmon in LHM Mediated Dielectric Gap Multilayer Structure," *Photonic Sensors*, 2020, 10(2): 113–122.

1. Introduction

Recently, metal-dielectric multilayer nanostructures supporting the propagation of surface plasmons (SPs) in appropriate conditions are currently investigated in the interest to assess particularly the limit of their specific sensitivity enhancement [1–3]. Generally, this performance parameter, which is requested to be high, is evaluated on the shift of the resonance condition with respect to any changes introduced in the refractive index (RI) of a sensing medium [4]. Generally, an interface performed between an infinite active metallic layer, such as silver (Ag), gold (Au), aluminum (Al), and a dielectric medium, once analyzed with p-polarized light beam via the attenuated total reflection (ATR) technique, exhibits an SP propagation. It should be noted that the angular resonance condition, of the generated SP mode, depends critically on both RIs and thicknesses of the whole associated media of the designed multilayer configuration [5–7]. Furthermore, the shift produced on the resonance peak and its line width evaluated on an interfacial SP profile were adopted as references to highlight the temperature effect [8], the carriers concentration of doped Si [9], percentages in nano-composite materials [10], the control of interface stability [11], and so on. Based on both the changes in resonance angles, $\theta_1 = \theta_{SPR}$ of the reflectance spectrum and its width, numerous types of geometries with appropriate choices of active materials have been reported in [7, 9, 12–15] and applied to wide uses such as gas detection [16, 17], medical diagnosis [18], and photonic devices [19]. By the use of graphene multilayer/Ag, Verma *et al*. [20] and

Received: 19 October 2018 / Revised: 28 May 2019

DOI: 10.1007/s13320-019-0568-3
Article type: Regular

Szunerits *et al.* [6] who also employed other strategies, succeeded in designing highly sensitive SPR sensors. Generally, in the design of SPR sensors, the sensing properties may be tuned in different limits that depend mainly on the whole of the parameters of involved active materials and the surrounding dielectrics [20–24]. In order to further improve the relative sensitivity, Ouyang *et al*. [25] used the advantages of stacking Si/MoS_2 under the Au layer exhibiting a single SPR mode whose full width at half maximum (FWHM) termed, $dq_{0.5}$ at 50 % of reflectivity, is significantly wider when increasing the number of MoS_2 layers. To produce a sharp and sensitive peak ascribed to coupled modes, Kullab *et al.* [26] proposed a novel four-layer scheme where a metamaterial (left-handed material and right-handed material) is included as a core layer to demonstrate that the designed structure presents an advantage over other optical sensors. It should be noted that the largest peak of the resonance condition, measured on angular reflectance spectra, constitutes a disadvantage for using the resonance angle as a key parameter in characterizing RI of aqueous solutions on the SPR sensors' surface [27, 28].

To manipulate the sensitivity in acceptable limits, recent research [29] adopted the strategies including the porosity effect in an SPR sensor to estimate the angular SPR curve and detect the accuracy (D.A=$1/\Delta\theta_{0.5}$) of 1.098/°. In order to maximize the sensing sensitivity, a slab waveguide structure, based on the air gap enclosed between anisotropic LHM layers operating in the microwave frequency range, has been explored for refractometry applications [30].

Here, in the purpose of improving the sensitivity in a different way, we investigate the sensing response of a planar multilayer structure disposed on a prism-coupler. We discuss the influence on both RI and the thickness of an inner core (sensing medium) included between the left-handed material and Au. Clear evidence of ultra-high sensitivity and specific behaviors are shown on the profiles of confined electromagnetic modes, depending on the incident angle, θ_1 of an excitation light, which has not been yet observed in metal-insulator-metal structures.

This paper is organized as follows. First, we describe the essential formulas of electromagnetic fields that propagate within the configuration under study and the enhancement factors (EFs). Second, we present the obtained results with significant interpretations. Finally, the paper ends with conclusions. The transfer matrix method (TMM), leading to simulate the p-reflectance profile, is repeated in the appendix section.

2. Field equations near flat interfaces of an SPR sensor

The multilayer structure under study is schematically illustrated in Fig. 1. The one dimensional (1D) planar nanocavity, deposited on a SiO_2 glass prism, is made up of a dielectric layer bounded by two active materials, LHM and Au. In the present work, the optical response was calculated for Au and LHM as an outermost layer. Besides, it is assumed that the in- and outer-most media extend to infinity. All the parameters of the multilayered structure are specified in Fig. 1. To create SP' mode, a continuous transverse magnetic (TM)-polarized light (under incident angle, θ_1) of fixed wavelength, λ, illuminates the multilayer structure through a SiO_2 glass prism.

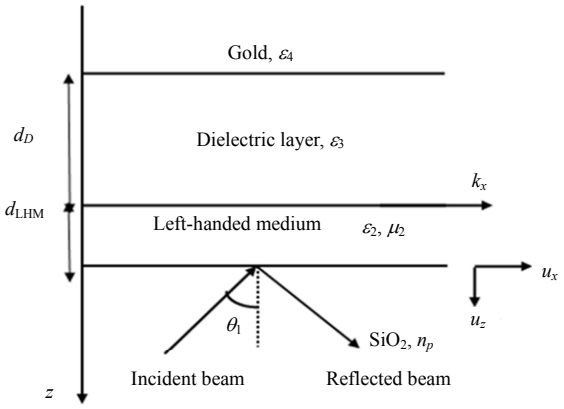

Fig. 1 Multilayer configuration under study: an LHM layer $(\varepsilon_2, \mu_2, d_{\mathrm{LHM}})$, a dielectric layer (ε_3, d_D), and an Au-bulk $\varepsilon_{\mathrm{Au}} = \varepsilon_4$, which are stacked along z-direction on a SiO_2 glass prism or RI, $\left(n_p = \sqrt{\varepsilon_p}\right)$.

Thus, assume the structure of Fig. 1, being oriented in *z*-axis, the incident beam, under the angle, $\theta_1 < \theta_{cr}$ (critical angle), is partially reflected and transmitted on either side of the interfaces. So, the explicit equations of all the electric fields propagating in each medium at the z-coordinate of the SPR approach: prism, LHM, dielectric layer, and Au, can be written as the following form:

$$E_p = \left\{ E_{1x} \begin{pmatrix} 1 \\ 0 \\ k_x / k_{z1} \end{pmatrix} \mathrm{e}^{\mathrm{i}\{k_x x + k_{z1}[z-(d_{\mathrm{LHM}}+d_D)]\}} \right\} \mathrm{e}^{-\mathrm{i}\omega t} \quad (1)$$

for $z \geq d_{\mathrm{LHM}} + d_D$, where E_{1x} denotes the electric field amplitude along the *x*-axis. Here, $k_x = \frac{2\pi}{\lambda}\sqrt{\varepsilon_p}\sin\theta_1$ is the wave vector component along the *x*-axis in the prism, and $k_{zj} = \frac{2\pi}{\lambda}\left(\varepsilon_i \mu_j - \varepsilon_p \sin^2\theta_1\right)^{1/2}$ denotes the wave vector component along the *z*-axis in each layer of the structure indexed, *j* with, *j* = 1, 2, 3, and 4, respectively:

$$E_{\mathrm{LHM}} = m\left\{ E_{1x} \begin{pmatrix} 1 \\ 0 \\ k_x / k_{z2} \end{pmatrix} \mathrm{e}^{\mathrm{i}\left[k_x x + k_{z2}\left(z-d_{\mathrm{LHM}}\right)\right]} \mathrm{e}^{-\mathrm{i}\omega t} \right\} \quad (2)$$

for $d_{\mathrm{LHM}} \geq z \geq d_D$, with

$$m = \frac{\left(1-r_{12}\right)\left(1-r_{23}\right)}{\mathrm{e}^{-\mathrm{i}k_{z2}d_{\mathrm{LHM}}} - r_{23}\mathrm{e}^{\mathrm{i}k_{z2}d_{\mathrm{LHM}}}}$$

and

$$E_D = m'\left\{ E_{1x} \begin{pmatrix} 1 \\ 0 \\ k_x / k_{z3} \end{pmatrix} \mathrm{e}^{\mathrm{i}\left[k_x x + k_{z3}\left(z-d_D\right)\right]} \mathrm{e}^{-\mathrm{i}\omega t} \right\} \quad (3)$$

for $d_D \geq z \geq 0$, with

$$m' = \frac{\left(1-r_{12}\right)\left(1-r_{23}\right)\left(1-r_{34}\right)}{\left(\mathrm{e}^{-\mathrm{i}k_{z1}d_{\mathrm{LHM}}} - r_{23}\mathrm{e}^{\mathrm{i}k_{z1}d_{\mathrm{LHM}}}\right)\left(\mathrm{e}^{-\mathrm{i}k_{z3}d_{\mathrm{LHM}}} - r_{34}\mathrm{e}^{\mathrm{i}k_{z3}D}\right)}$$

and

$$r_{12} = \frac{1-b_1}{1+b_1},\ r_{23} = \frac{1-b_2}{1+b_2},\ r_{34} = \frac{1-b_3}{1+b_3}$$

are the reflection coefficients of the structure interfaces.

$$E_{Au} = m'\left\{ E_{1x} \begin{pmatrix} 1 \\ 0 \\ k_x / k_{z4} \end{pmatrix} \mathrm{e}^{\mathrm{i}(k_x x + k_{z4} z)} \right\} \mathrm{e}^{-\mathrm{i}\omega t} \quad (4)$$

for $z \leq 0$, with

$$b_1 = \frac{k_{z2}\varepsilon_p\left(1-\mathrm{e}^{2\mathrm{i}k_{z2}d_{\mathrm{LHM}}}\right)}{k_{z1}\varepsilon_{\mathrm{LHM}}\mu_{\mathrm{LHM}}\left(1+\mathrm{e}^{2\mathrm{i}k_{z2}d_{\mathrm{LHM}}}\right)}$$

$$b_2 = \frac{k_{z3}\varepsilon_{\mathrm{LHM}}\left(1-\mathrm{e}^{2\mathrm{i}k_{z3}d_D}\right)}{k_{z2}\varepsilon_3\left(1+\mathrm{e}^{2\mathrm{i}k_{z3}d_D}\right)}$$

and $b_3 = \frac{\varepsilon_3 k_{z4}}{\varepsilon_4 k_{z3}}$.

In a similar form of (1)–(4), the associated magnetic fields *B* propagating through the proposed four-layer sensor, can be easily determined by the usual Maxwell equation:

$$\nabla \times E + \frac{\partial B}{\partial t} = 0.$$

The above set of (1)–(4) is the starting point to carry out a comprehensive analysis on the propagation of the guided resonant modes according to both directions, u_x and u_z, when a monochromatic wave irradiates the structure under an incidence angle θ_1 beyond θ_{cr}. In this condition, and for an adjusted LHM layer thickness, d_{LHM}, most of the incident energy is absorbed by the layered materials and generates SPs at the boundary LHM-dielectric layer interface. As indicated in the example geometry of Fig. 1, the supported SP modes will be studied in the two possible arrangements between LHM and Au separated by a dielectric layer (sensing medium). Thus, in our theoretical simulation, the chosen parameters of the active material layers are described by the complex permittivity, $e_{\mathrm{Au}}(\mathrm{l})$= –21.3+i1.35 for gold, which is taken from [31], and $\varepsilon_2(\lambda) = -33.5$, $\mu_2(\lambda) = -11$ for LHM [32], which are evaluated at operating wavelength of λ=738 nm. Refractive indices for SiO_2-glass prism and sensing medium are $n_p = \sqrt{\varepsilon_p} = 1.57$ and $n_3 = \sqrt{\varepsilon_3} = 1.46$, respectively.

According to the *xz*-plane, the resulting interfacial modes, selected along u_x and u_z directions, can be described through the following longitudinal and perpendicular confinement factors

as follows, respectively:

$$f_{\parallel}(\theta_1)=\frac{\left|E_{\mathrm{Au}}u_x\right|_{z=0}}{\left|E_p u_x\right|_{z=d_D}}=m' \tag{5}$$

$$f_{\perp}(\theta_1)=\frac{\left|E_{Au}u_z\right|_{z=0}}{\left|E_p u_z\right|_{z=d_D}}=\frac{k_{z1}}{k_{z4}}m \tag{6}$$

whose characteristics, therefore, are considered for the analytical resolution in terms of sensitivity (extracted from angular reflectance spectra) of the proposed SPR sensor on both the thicknesses of LHM (d_{LHM}) and dielectric layer d_D.

3. Physics of surface plasmons

Surface plasmons are basically collective oscillating charges that propagate along a thin metallic layer bounded by a dielectric medium with electric field decaying exponentially, i.e., the evanescent character, in both the media. Otherwise, SPs occur when an incident p-polarized light of a given wavelength strikes the metallic surface at an angle, $\theta_1 > \theta_{\mathrm{cr}}$ through the coupling prism (or metallic grating). Under these conditions, the light reflectivity from the prism base reduces to the minimum due to the plasmonic absorption mechanism. The position of this particular angle, θ_1, called the angular resonance of SP and the width at 50% of the reflected light profile, can be substantially affected with little variation in the optical constants of associated media of the proposed device. This effect is due to the presence of the evanescent field surrounding the active metamaterial (LHM). So, due to these effects, it should be necessary to investigate the sensitivity by combining different electromagnetic properties of conducting materials as LHM and Au with dielectric substrates. It is to be mentioned here that the choice of Au comes from the fact that it presents favorable properties over other metals.

4. Results and discussion

First, to investigate the potential of the proposed SPR nanocavity formed with a dielectric layer of RI $\left(n_D=\sqrt{\varepsilon_D}\right)$ and surrounded by a LHM layer (e_2, m_2) and a bulk-LHM, we plot the reflectance curve versus incidence angle, as shown in Fig. 2. This interfacial response is calculated from the transfer matrix method (TMM) which was previously detailed elsewhere [22].

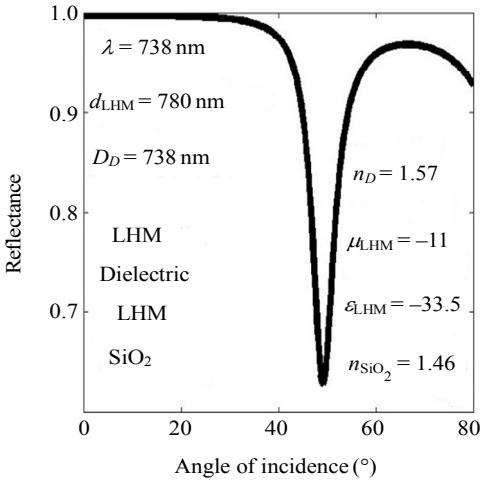

(b)

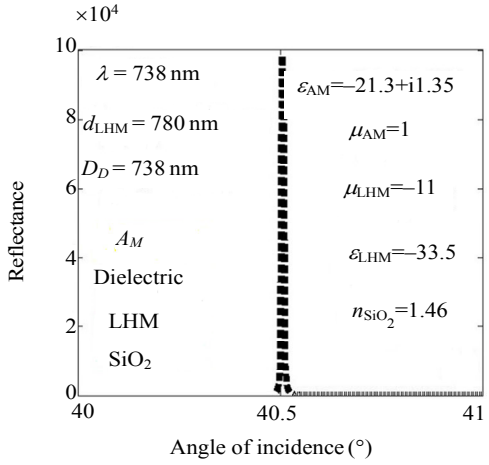

(b)

Fig. 2 Calculated angular P-reflectance spectra investigated from the samples: (a) prism-LHM layer- dielectric gap layer-LHM bulk, and (b) prism-LHM-dielectric gap layer-Au bulk. The parameter conditions are specified in the inset of the figures.

The formalism of TMM, applied to the proposed SPR nanocavity with a prism-coupler, is repeated in the appendix section of the paper. For the stacking shown in the inset of Fig. 2(a), by considering the thicknesses, 780 nm and 330 nm of LHM layer and dielectric, respectively, the (1D)-nanocavity exhibits a single SPR mode excited at 49.23°. These

optimized thicknesses are necessary to achieve the lowest point of the minimum p-reflectance curve of 62%. For this resolved peak-SPR mode in the angular p-reflectance curve, the estimation of quality factor $Q = \theta_{SPR} / \Delta\theta_{0.5}$ reaches the value of $12 \left(\Delta\theta_{0.5} = 5.58° \right)$. In the case, where Au is taken as an outermost layer, [see Fig. 2(b)], the p-reflectance curve shows the existence of a single peak-SPR mode at the angle of θ_{SPR} = 40.51° whose intensity achieves a maximum value of ~9.85×10^4. From a systematic comparison between the results of Figs. 2(a) and 2(b) in terms of the reflectance intensities, it means that Au, with a loss tangent angle 0.063 as an outermost layer when combined with the LHM layer, causes a substantial optical amplification of an extremely narrow full width at half maximum (FWHM). The resonant modes sustained by the interfaces within the dielectric layer (sensing layer) can be coupled to each other and make more energy stored on the outermost medium (Au). This effect, being resulted from the optical coupling process generated between electromagnetic modes inside the designed (1D)-nanocavity, has been recently observed experimentally by Hayashi *et al*. [33] and Goswami *et al*. [34] in other variant SPR systems. According to the above quantitative characteristics related to the SP' excitation, the proposed device exhibits a significant application as a tunable filter.

Next, we discuss theoretically the effects induced in the resonance (ATR) intensity on both the thicknesses of LHM, d_{LHM} and the dielectric layer, d_D. The structure being considered here concerns the arrangement as: SiO_2 prism/LHM(d_{LHM})/dielectric gap (d_D)/Au-bulk. As a result, with a fixed thickness, d_D =330 nm [see Fig. 3(a)], by tuning the thickness, d_{LHM} from 779.6 nm to 780.4 nm, a dominant amplification of ~9.85×10^4 arises at 40.51° for d_{LHM}=780 nm. Taking this condition, the above amplification value may be further optimized [see Fig. 3(b)] by increasing against the thickness d_D around the range of 329 nm to 333 nm. The p-reflectance peak of the exhibited SPR mode gets a value in the order of 2.13×10^6 estimated at the resonance angle of 40.74°. Such an optimization fulfilling to the condition, $d_D/(d_D+d_{LHM})$~0.3 leads to highlight that the thickness of the LHM layer, and the one of the dielectric layer of a fixed RI, n_D, plays an essential way for producing a sharper optical amplification that can be exploited in an SPR sensing purpose. It is worth noting that the effect on RI, n_D of the dielectric layer, was discussed in our previous work [22].

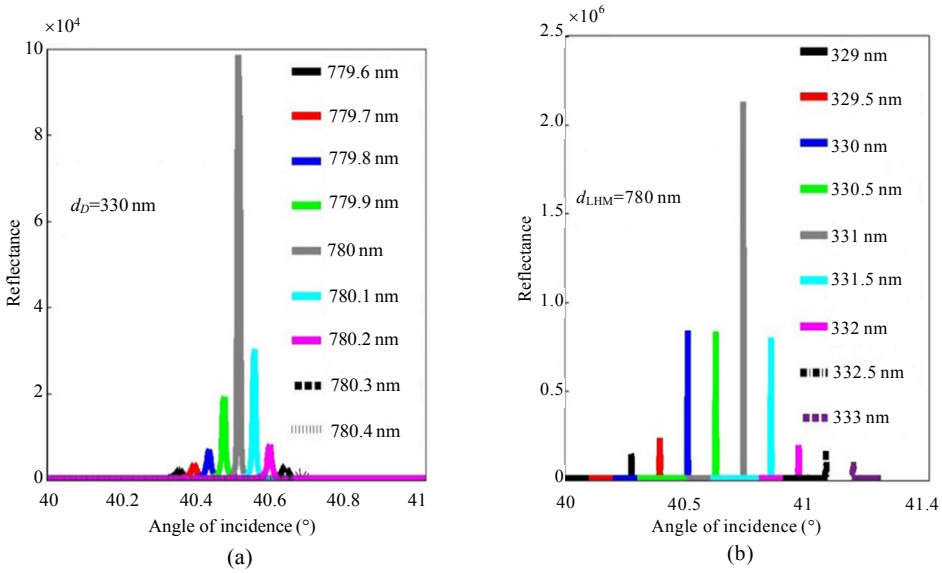

Fig. 3 Angular p-reflectance spectra for the arrangement prism/LHM/Dielectric layer/Au, when changing (a) for different LHM layer thickness from 779.6 nm to 780.4 nm with a fixed dielectric layer set to be 330 nm, and (b) for different dielectric layer thickness from 329 nm to 333 nm with a fixed LHM thickness set to be 780 nm.

In this part, we put now emphasis on the characteristics evaluated on the enhancement factors (EFs) curves, $f_{\perp}$ and $f_{\parallel}$ previously defined in Figs. 7(a) and 7(b). Therefore, in the optimized condition of Fig. 3(a), i.e., with d_D= 330 nm and d_{LHM}=780 nm, the angular dependencies of $f_{\perp}$ and $f_{\parallel}$ in the large angular range from 33° to 73° are depicted in Figs. 4(a) and 4(b), respectively. On the angular profile of each curve, the total thickness, $d = (d_D + d_{LHM})$=1110 nm, gives the ability of generating simultaneously two sharper confined modes (associated to the supported SPs) at the resonance angles 33.83°(first-mode), and 72.22° (second-mode). Moreover, it should be noted that the two EFs' profiles through the structure present the same stop-band defined between the successive confined modes. The narrowest peak intensities of these confined modes for $f_{\parallel}$ are slightly different, i.e., 0.8×10^6 and 1.35×10^6, except for the ones of $f_{\perp}$, there is rather a notable difference, 3.09×10^6 and 0.15×10^6. So, the multilayer structure: SiO_2 prism/LHM (780 nm)/dielectric gap (330 nm)/ Au-bulk sustains a giant amplification as reported in Fig. 2(b), and consequently, the structure characterized by the highest EFs is very promising to develop bio-sensing applications. For a comparison, recently, Sekkat *et al.* [24] proposed Ag/Cytop interfaces as a plasmonic planar structure leading to achieving a giant amplification~1.3×10^6, which remains much less than the one we obtained here.

Following the above analysis, we finally focus on simulating the relationships between the angular resonances, θ_{SPR} with the variation of thicknesses, d_D and d_{LHM} of the EFs intensities as shown in Fig. 4. Thus, based on typical curves as depicted in Fig. 4(a), when we consider the thickness, d_D fixed at 330 nm, it is observed that the resonance condition, θ_{SPR} of each mode in the EF curve of $f_{\perp}$ increases sensitively with an increase in d_{LHM} from 779.6 nm to 780.4 nm [see Figs. 5(a) and 5(b)]. From these data, the observed change in SPR angle θ_{SPR} as a function of the LHM thickness, d_{LHM}, can be numerically predicted as:

$$\theta_{SPR,\perp}(d_{LHM}) = 1.1195 d_{LHM}^3 - 2623.9 d_{LHM}^2 + 2.05\times10^6 d_{LHM} - 5.34\times10^8 \pm 0.029°. \quad (7)$$

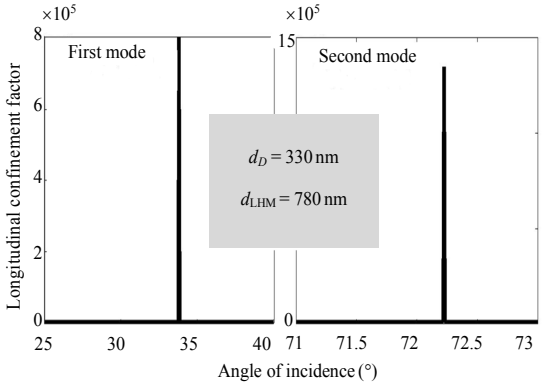

(a)

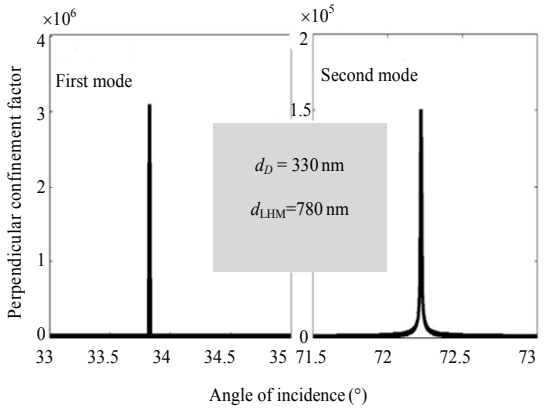

(b)

Fig. 4 Angular dependency of the interface' modes displayed on (a) the perpendicular and (b) the longitudinal confinement factors, $f_{\perp}$ and $f_{\parallel}$ in the arrangement: prism-LHM-dielectric gap layer-Au outermost medium, with an LHM layer set to be 780 nm., and dielectric layer is set to be 330 nm. The other medium parameters are the same as those reported in the inset of Fig. 2(b).

For the same purpose, by considering the thickness d_{LHM} fixed at 780 nm, the resonance condition θ_{SPR} of each mode in the EF curve of, $f_{\perp}(\theta)$ increases linearly with an increase in the thickness d_D from 329 nm to 333 nm [see Figs. 5(c) and 5(d)]. Therefore, this dependency, in this condition, can be analytically predicted from the following form:

$$\theta_{SPR,\perp}(d_D) = (0.17867 \times d_D - 25.13°) \pm 0.0078° \quad (8)$$

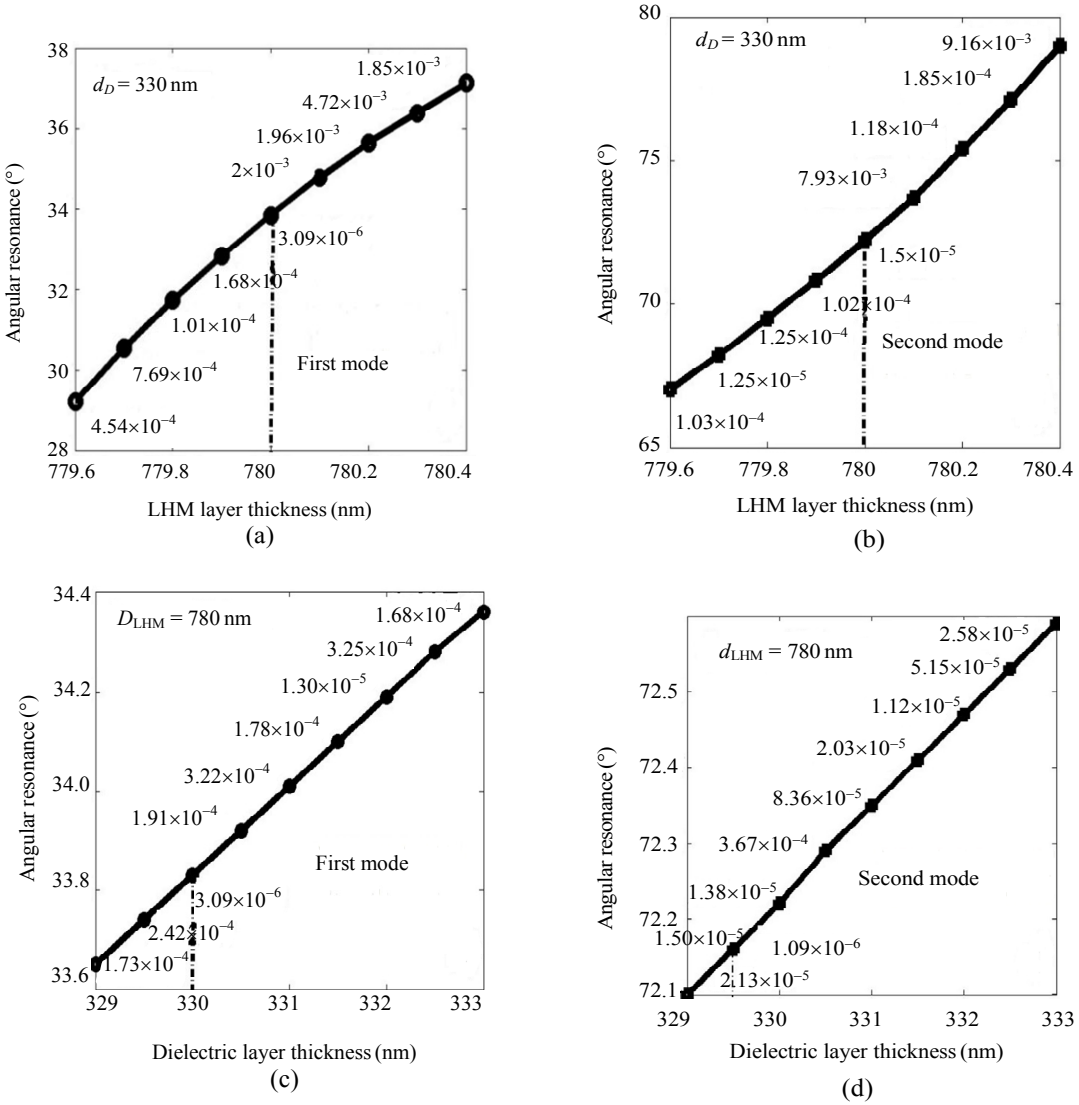

Fig. 5 Evolution in the SPR angle for: (a) the first-confined mode, (b) the second-confined mode displayed on the perpendicular enhancement factor, $f_{\perp}$ under the change of the LHM thickness with a fixed dielectric layer, d_D=330 nm, (c) first-confined mode, and (d) second-confined mode displayed on the perpendicular enhancement factor, $f_{\perp}$ under the change of the dielectric layer thickness with a fixed, metamaterial layer, d_{LHM}=780 nm.

A similar study has been conducted on the evolution of each mode in the EF curve of $f_{//}$ versus d_{LHM} and d_d. By taking into account typical curves as shown in Fig. (4), the extracted data are represented in Figs. 6(a)–6(d). For the two cases considered separately, it is observed that for each EF' mode of $f_{\parallel}$, their respective resonance condition increases with an increase in either d_{LHM} or d_D. Thus, for each condition, such a dependency in the SPR condition of $f_{//}$ curve versus d_{LHM} or d_D can be predicted, respectively, by the following relations:

$$\theta_{SPR,\parallel}(d_{LHM}) = 1.1195 d_{LHM}^3 - 2801.2 d_{LHM}^2 + 2.1882\times10^6 d_{LHM} - 5.6979\times10^8 \quad (9)$$

$$\theta_{SPR,\parallel}(d_D) = 0.1796 \times d_D - 25\,. \quad (10)$$

In Figs. 5 and 6, the reported values on these curves represent the achieved intensities of EF modes according to the relative values of the thicknesses d_D and d_{LHM}.

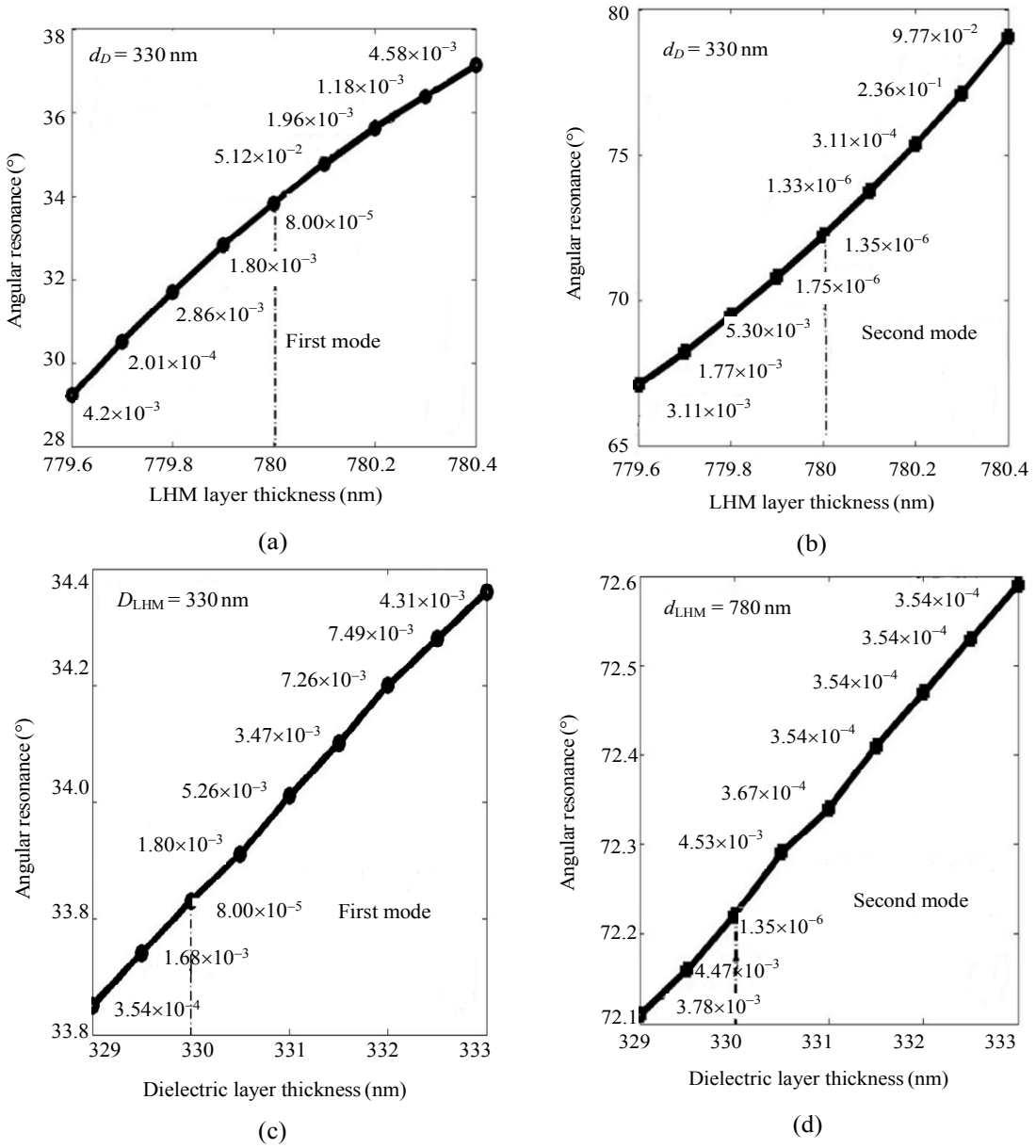

Fig. 6 Evolution in the SPR angle for: (a) first-confined mode and (b) second-confined mode displayed on the parallel enhancement factor $f_{\|}$ under the change of LHM thickness with a fixed d_D=330 nm, (c) first-confined mode, and (d) second-confined mode displayed on the parallel enhancement factor $f_{\|}$ under the change of dielectric gap with a fixed thickness, d_{LHM}=780 nm.

5. Conclusions

In this paper, a plasmonic sensor, with an active LHM layer of simultaneous negative permittivity and permeability, stacked on a dielectric layer and Au, has been investigated theoretically. This SPR sensor, based on gold (Au) taken as an outermost medium, has the capability of exhibiting substantial electromagnetic modes confined on the structure' interfaces. However, the resulting optical amplification predicted on both the longitudinal and perpendicular factors due to the existence of resonant modes with narrower angular widths, depends critically on the ratio evaluated between the structure' thicknesses. It has been observed that the characteristics (peak intensity, resonance angle, and line width) of the SPR modes probed in an angular interrogation method can be highly controlled on the change of the dielectric gap thickness of fixed refractive index. Based on the

electromagnetic calculations, the giant optical amplification ~3.09×10^6 of exhibited mode on the interfaces of the proposed device, is highly sensitive to the ratio defined between the structure thicknesses $d_D/(d_D+d_{\mathrm{LHM}})$ and it can be constituted as a new limit which is even greater than the one of conventional SPR sensors for developing photonic applications.

Appendix A

Since the proposed planar SPR sensor displayed in the arrangement of Fig. 1 is comprised of four layers stacked along the *z*-axis, its corresponding angular p-reflectance accordingly to the TMM is given as

$$\left|R_p\left(\theta_i\right)\right|^2=\left|\frac{\left(M_{11}+M_{12}q_4\right)q_1-\left(M_{21}+M_{22}q_4\right)}{\left(M_{11}+M_{12}q_4\right)q_1+\left(M_{21}+M_{22}q_4\right)}\right|^2. \quad \text{(A1)}$$

In above (A1), M_{ij} elements, for $i = j$ =1, 2, satisfy the following expressions:

$$M_{11}=\left(1+\frac{q_3}{q_2}\tan\beta_2\tan\beta_3\right)\prod_{k=2}^{3}\cos\beta_k \quad \text{(A2)}$$

$$M_{12}=-\mathrm{i}\left(\frac{1}{q_3}+\frac{1}{q_2}\frac{\tan\beta_2}{\tan\beta_3}\right)\cos\beta_2\sin\beta_3 \quad \text{(A3)}$$

$$M_{21}=-\mathrm{i}\left(q_2+q_3\times\frac{\tan\beta_3}{\tan\beta_2}\right)\sin\beta_2\cos\beta_3 \quad \text{(A4)}$$

$$M_{22}=\left(1+\frac{q_2}{q_3}\tan\beta_2\tan\beta_3\right)\prod_{k=2}^{3}\cos\beta_k \quad \text{(A5)}$$

with

$$\begin{cases}\beta_2=\dfrac{2\pi d_{\mathrm{LHM}}}{\lambda}\left(\varepsilon_2\mu_2-\varepsilon_p\sin^2\theta_1\right)\\ \beta_3=\dfrac{2\pi d_D}{\lambda}\left(\varepsilon_3-\varepsilon_p\sin^2\theta_1\right)\end{cases} \quad \text{(A6)}$$

where $\mathrm{i}=\sqrt{-1}$ is the imaginary complex. The terms q_n for n =1, 2, 3, 4 corresponding to the wave vector compounds along the *z*-axis in prism (SiO_2), LHM layer, sensing medium layer (dielectric), and outermost medium (Au), respectively, are expressed as

$$\begin{cases}q_1=\left(\dfrac{1}{\varepsilon_p}\right)^{1/2}\cos\theta_1,\ q_2=\dfrac{1}{\varepsilon_2}\left(\varepsilon_2\mu_2-\varepsilon_p\sin^2\theta_1\right)^{1/2}\\ q_3=\dfrac{1}{\varepsilon_3}\left(\varepsilon_3-\varepsilon_p\sin^2\theta_1\right)^{1/2},\ q_4=\dfrac{1}{\varepsilon_4}\left(\varepsilon_4-\varepsilon_p\sin^2\theta_1\right)^{1/2}.\end{cases} \quad \text{(A7)}$$

Hence, to extract the performance parameters as previously discussed, in the adopted approach of four layers, p-reflectance, (A1) at the prism-active material interface is to be exploited analytically versus incidence angle θ_i for a fixed wavelength λ of incident beam.

References

[1] A. Verma, A. Prakash, and R. Tripathi, "Sensitivity enhancement of surface plasmon resonance biosensor using graphene and air gap," *Optics Communications*, 2015, 357: 106–112.

[2] O. Saison-fransioso, G. Lévêque, A. Akjouj, Y. Pennec, B. Djafari-rouhani, S. Szunerits, *et al.*, "Plasmonic nanoparticules arrays for high-sensitivity sensing: a theoretical investigation," *The Journal of Physical Chemistry C*, 2012, 116(33): 17819–17827.

[3] M. S. Rahman, M. S. Anower, L. B. Bashar, and K. A. Rikta, "Sensitivity analysis of grapheme coated surface plasmon resonance biosensors for biosensing applications," *Sensing and Bio-sensing Research*, 2017, 16: 41–45.

[4] A. K. Sharma, R. Jha, and B. D. Gupta, "Fiber-optic sensors based on surface plasmon resonance: a comprehensive review," *IEEE Sensors Journal*, 2007, 7(8): 1118–1129.

[5] A. Shalabney, C. Khare, B. Rauschenbach, and I. Abdulhalim, "Sensitivity of surface plasmon resonance sensors based on metallic columnar thin films in the spectral and angular interrogations," *Sensors and Actuators B*: *Chemical*, 2011, 159(1): 201–212.

[6] S. Szunerits, X. Castel, and R. Boukherroub, "Surface plasmon resonance investigation of silver and gold films coated with thin indium tin oxide layers: influence on stability and sensitivity," *The Journal of Physical Chemistry C*, 2008, 112(40): 15813–15817.

[7] S. A. Taya and H. M. Kullab, "Optimization of transverse electric peak-type metal clad waveguide sensor using double-negative materials," *Applied Physics A*, 2014, 116(4): 1841–1846.
[8] H. P. Chiang, C. W. Chen, J. J. Wu, H. L. Li, T. Y. Lin, E. J. Sanchez, *et al.*, "Effects of temperature on the surface plasmon resonance at a metal-semiconductor interface," *Thin Solid Films*, 2007, 515(17): 6953–6961.
[9] B. Bouhafs, M. Benatallah, and M. Bendjebbour, "Resonant electromagnetic field distribution on doped multilayer thin film structure," *Spectroscopy Letters*, 2014, 47(5): 397–403.
[10] H. Deng, D. Yang, B. Chen, and C. Lin, "Simulation of surface plasmon resonance of Au-WO_{3-x} and Ag-WO_{3-x} nanocomposite films," *Sensors and Actuators B: Chemical*, 2008, 134(2): 502–509.
[11] S. Szunerits, X. Castel, and R. Boukherroub, "Preparation of electrochemical and surface plasmon resonance active interfaces: deposition of indium tin oxide on silver thin films," *The Journal of Physical Chemistry C*, 2008, 112(29): 10883–10888.
[12] Y. Yuan and Y. Dai, "A revised LRSPR sensor with sharp reflection spectrum," *Sensors*, 2014, 14(9): 16664–16671.
[13] T. Vary and P. Markos, "Propagation of surface plasmon polaritons through gradient index and periodic structures," *Opto-Electronics Review*, 2010, 18(4): 400–407.
[14] R. Slavik and J. Homola, "Simultaneous excitation of long and short range surface plasmons in an asymmetric structure," *Optics Communications*, 2006, 259(2): 507–512.
[15] L. Shen and Z. Wang, "Guided modes in a four-layer slab waveguide with dispersive left-handed material," *Journal of Electromagnetic Analysis and Applications*, 2010, 2(04): 264.
[16] C. Nylander, B. Liedberg, and T. Lind, "Gas detection by means of surface plasmon resonance," *Sensors and Actuators*, 1982, 3: 79–88.
[17] K. Lin, Y. Lu, J. Chen, R. Zheng, P. Wang, and H. Ming, "Surface plasmon resonance hydrogen sensor based on metallic grating with high sensitivity," *Optics Express*, 2008, 16(23): 18599–18604.
[18] J. W. Chung, S. D. Kim, R. Bernhardt, and J. C. Pyun, "Application of SPR biosensor for medical diagnostics of human hepatitis B virus (hHBV)," *Sensors and Actuators B*: *Chemical*, 2005, 111: 416–422.
[19] K. Wen, L. Yan, W. Pan, B. Luo, Z. Guo, Y. Guo, *et al*., "Design of plasmonic comb-like filters using loop-based resonators," *Plasmonics*, 2013, 8(2): 1017–1022.
[20] A. Verma, A. Prakash, and R. Tripathi, "Sensitivity enhancement of surface plasmon resonance biosensor using graphene and air gap," *Optics Communications*, 2015, 357: 106–112.
[21] S Pal, Y. K. Prajapati, J. P. Saini, and V. Singh, "Sensitivity enhancement of metamaterial- based surface plasmon resonance biosensor for near infrared," *Optica Applicata*, 2016, 46(1): 131–143.
[22] A. Cherifi and B. Bouhafs, "Potential of SPR sensors based on multilayer interfaces with gold and LHM for biosensing applications," *Photonic Sensors*, 2017, 7(3): 199–205.
[23] S. Hayashi, D. V. Nesterenko, A. Rahmouni, H. Ishitobi, Y. Inouye, S. Kawata, *et al.*, "Light-tunable Fano resonance in metal-dielectric multilayer structures," *Scientific Reports*, 2016, 6: 33144.
[24] Z. Sekkat, S. Hayashi, D. V. Nesterenko, A. Rahmouni, S. Refki, H. Ishitobi, *et al*., "Plasmonic coupled modes in metal-dielectric multilayer structures: Fano resonance and giant field enhancement," *Optics Express*, 2016, 24(18): 20080–20088.
[25] Q. Ouyang, S. Zeng, X. Dinh, P. Coquet, and K. Yong, "Sensitivity enhancement of MoS_2 nanosheet based surface plasmon resonance biosensor," *Procedia Engineering*, 2016, 140: 134–139
[26] H. M. Kullab, S. A. Taya, and T. M. El-Agez, "Metal-clad waveguide sensor using a left-handed material as a core layer," *Journal of the Optical Society of America B*, 2012, 29(5): 959–964.
[27] Q. Ouyang, S. Zeng, L. Jiang, L. Hong, G. Xu, X. Dinh, *et al*., "Sensitivity enhancement of transition metal dichalcogenides/silicon nanostructure-based surface plasmon resonance biosensor," *Scientific Reports*, 2016, 6: 28190.
[28] A. K. Sharma, "Model of a plasmonic phase interrogation probe for optical sensing of hemoglobin in blood samples," *Sensing and Imaging*, 2015, 16(1): 10.
[29] Q. Meng, X. Zhao, C. Lin, S. Chen, Y. Ding, and Z. Chen, "Figure of merit enhancement of a surface plasmon resonance sensor using a low-refractive-index porous silica film," *Sensors*, 2017, 17(8): 1846.
[30] S. A. Taya, "Slab waveguide with air core layer and anisotropic left-handed material claddings as a sensor," *Opto-Electronics Review*, 2014, 22(4): 252–257.
[31] A. D. Rakic´, A. B. Djurisic´, J. M. Elazar, and M. L. Majewski, "Optical properties of metallic films for vertical-cavity optoelectronic devices," *Applied Optics*, 1998, 37(22): 5271–5283.
[32] S. M. Xiao, V. P. Drachev, A. V. Kildishev, X. J. Ni, U. K. Chettiar, H. K. Yuan, *et al.*, "Loss-free and active optical negative-index metamaterials," *Nature*, 2010, 466(7307): 735.
[33] S. Hayashi, D. V. Nesterenko, and Z. Sekkat, "Waveguide-coupled surface plasmon resonance sensor structures: Fano lineshape engineering for ultrahigh-resolution sensing," *Journal of Physics D: Applied Physics*, 2015, 48(32): 325303.
[34] N. Goswami, A. Saha, and A. Ghosh, "Optical amplification with surface plasmon resonance and total internal reflection in gold nanostructure with BK7 parallel slab," *International Journal of Chemtech Research*, 2014, 7(3): 1148–1153